AIP Physics of Fluids

Smallangle multiple scattering of charged particle beams

Thomas P. Hughes and Brendan B. Godfrey

Citation: Physics of Fluids (1958-1988) **27**, 1531 (1984); doi: 10.1063/1.864786
View online: http://dx.doi.org/10.1063/1.864786
View Table of Contents: http://scitation.aip.org/content/aip/journal/pof1/27/6?ver=pdfcov
Published by the AIP Publishing

Small-angle multiple scattering of charged particle beams

Thomas P. Hughes and Brendan B. Godfrey
Mission Research Corporation, Albuquerque, New Mexico 87106

(Received 28 December 1983; accepted 24 February 1984)

The scattering of self-pinched particle beams propagating in gas is investigated using Moliere's treatment of multiple scattering. Nordsieck lengths significantly longer than those predicted on the basis of less accurate scattering formalisms are obtained numerically. An improved analytic expression for the Nordsieck length is derived and agrees well with the numerical results. Experimental data on beam expansion from the ASTRON experiment show good agreement with numerical simulations and analytic results. The evolution of a thin annular beam due to scattering is studied, and the beam is found to acquire a Bennett profile in a distance on the order of one Nordsieck length.

I. INTRODUCTION

When a self-pinched particle beam propagates through a gas, it undergoes multiple scattering off background nuclei. As a result, the mean radius of the beam tends to increase and the mean beam density decreases. In this paper we show that the expressions presently used to compute the rate of expansion of the beam are inaccurate at low beam power. This is because these expressions are based on an approximate Fokker–Planck treatment of multiple small-angle scattering which is not appropriate for self-pinched beams. In Sec. II we point out the problems involved in this treatment and describe a more accurate treatment based on the Moliere formulation of multiple scattering. We show how a numerical algorithm is constructed to implement this improved treatment in a particle simulation code. In Sec. III, we give the results of numerical computations of Nordsieck length (the distance for one e-folding in beam radius) as a function of beam power, using a simple particle code SCATR (see the Appendix). On the basis of these results, we carry out a semi-analytical derivation of an expression for the Nordsieck length of a Bennett profile beam.[1,2] In Sec. IV we compare numerical and analytical results with experimental data for the ASTRON electron beam. Good agreement is obtained. In Sec. V, we examine the evolution of a non-Bennett equilibrium (an annular beam) and show that it becomes Bennett-like in about one Nordsieck length. We summarize our conclusions in Sec. VI.

II. THEORY OF MULTIPLE SMALL-ANGLE SCATTERING

When a charged particle passes through a medium made up of identical scattering centers, the number of scattering events which it undergoes in traveling a distance z is

$$N_0 \approx 2\pi n z \int_0^\infty \sigma(\theta)\theta\, d\theta, \tag{1}$$

where n is the number density of scattering centers, θ is the scattering angle, and $\sigma(\theta)\theta$ is the differential cross section. In writing Eq. (1) we have made the assumptions that $\sigma(\theta)$ is strongly peaked around $\theta = 0$ and that the net deflection of the incident particle is small (much less than a radian) so that the path of the incident particle is approximately a straight line. When $N_0 \gg 1$, we are in multiple scattering regime.

A. Fokker–Planck formalism

To describe the behavior of a large number of incident particles, we use a distribution function $f(\mathbf{r}_\perp, \mathbf{p}_\perp, t)$, where $\mathbf{r}_\perp, \mathbf{p}_\perp$ are the transverse phase space coordinates of the beam of particles. The longitudinal displacement of the particles is assumed to be given by $z = vt$, where $v \approx c$, the velocity of light, is the beam velocity. The distribution function obeys the transport equation

$$\left(\frac{\partial f}{\partial t}\right)_{z=vt} + \frac{\mathbf{p}_\perp}{\gamma m}\cdot\frac{\partial}{\partial \mathbf{r}_\perp} f + \frac{d\mathbf{p}_\perp}{dt}\cdot\frac{\partial}{\partial \mathbf{p}_\perp} f = \left(\frac{\partial f}{\partial t}\right)_{\text{coll}} \equiv -2\pi n v f \int \sigma(\chi)\chi\, d\chi + 2\pi n v \int f(\boldsymbol{\theta} - \boldsymbol{\chi})\sigma(\chi) d\boldsymbol{\chi}, \tag{2}$$

where $d\mathbf{p}_\perp/dt$ is the force due to self-fields, $\boldsymbol{\theta}$ is a vector in the transverse plane related to $\mathbf{p}_\perp$ by $\boldsymbol{\theta} = \mathbf{p}_\perp/\gamma mc$, m is the electron mass, and $\gamma = (1 - v^2/c^2)^{-1/2}$. For many purposes, the Fokker–Planck treatment of the collision operator on the right-hand side is adequate. This consists of an expansion to second order in χ yielding

$$\left(\frac{\partial f}{\partial t}\right)_{\text{coll}} = \frac{1}{4}\langle \dot{\chi}^2\rangle \left(\frac{\partial^2 f}{\partial \theta^2} + \frac{1}{\theta}\frac{\partial f}{\partial \theta}\right), \tag{3}$$

where

$$\langle \dot{\chi}^2\rangle = 2\pi n v \int_0^\infty \chi^3\, d\chi\, \sigma(\chi).$$

The small-angle Rutherford cross section for an electron scattering off a nucleus is

$$2\pi\sigma(\chi)\chi\, d\chi = \frac{8\pi Z(Z+1)}{\beta^4\gamma^2}\left(\frac{e^2}{mc^2}\right)^2 \frac{\chi\, d\chi}{\chi^4} \equiv \frac{2\alpha^2\chi\, d\chi}{\chi^4}, \tag{4}$$

where $-e$ is the electron charge, Ze the nuclear charge, and $\beta = v/c$. Substituting this into Eq. (3), we find that the integral for $\langle \dot{\chi}^2\rangle$ is improper at both the lower and upper limits of integration. The divergence at the lower limit is due to the long range of the bare Coulomb potential. A suitable cutoff

 0031-9171/84/061531-07$01.90

can be introduced by taking account of the screening effect of atomic electrons. For the Thomas–Fermi atomic model, for example, one obtains[3] the lower bound $\theta_{\min} = \lambdabar/a \equiv \lambdabar/(0.885 a_0 Z^{-1/3})$, where $\lambdabar$ is the deBroglie wavelength of the incident electron, and a_0 is the Bohr atomic radius.

The divergence at the upper limit is an artifact of the small-angle approximation used, since a particle cannot scatter through an angle greater than π. The Fokker–Planck equation can be derived only in the small angle limit, however, so that one can either (a) introduce some "reasonable" upper bound on the scattering angle or (b) use a different treatment of small-angle scattering. Two commonly used upper bounds are $\theta_{\max} = 1$ for low electron energies ($\gamma < 100$) and $\theta_{\max} = \lambda / R_N$, where R_N is the nuclear radius, used by Rossi and Greisen, for high energies[4] ($\gamma > 100$). Using either of these, one can solve Eq. (2) analytically for certain initial conditions.[3,5] For future reference, we give the results for two cases.

1. Noninteracting particles

Assume the incident beam to have infinite transverse extent with $\partial/\partial \mathbf{r}_\perp \equiv 0$ and let $f \propto \delta(\mathbf{v}_\perp)$ at $t = 0$. The solution to Eqs. (2) and (3) is then

$$f(\theta, z) \propto \exp[-\theta^2/\langle \dot{\chi}^2 \rangle z]. \tag{5}$$

Since $\langle \chi^2 \rangle = 2n\alpha^2 \ln(\theta_{\max}/\theta_{\min})$ is a constant, the beam acquires a Maxwellian distribution in transverse velocity whose temperature increases linearly with the distance propagated.

2. Self-pinched Bennett-profile beam

From Eqs. (2) and (3), Lee[2] has shown that a Bennett-equilibrium beam expands self-similarly due to scattering with Bennett radius

$$R(z) = R_0 \exp(z/L_{\mathrm{N}}), \tag{6}$$

where L_{N} is the so-called Nordsieck length. Equation (6) is valid as long as the beam expansion is quasistatic, i.e., $v/L_{\mathrm{N}} \ll \omega_\beta(R)$, where $\omega_\beta \approx (\nu/\gamma)^{1/2} c/R$ is the mean betatron frequency, and ν is Budker's parameter (current divided by 17 kA). The expression obtained for L_{N} is

$$L_{\mathrm{N}} = \frac{\nu\gamma}{n\gamma^2\alpha^2 \ln(\theta_{\max}/\theta_{\min})}. \tag{7}$$

Here and subsequently, ν is a measure of the *net* current flowing. The plasma return current, if any, is assumed to have the same profile as the beam current. Taking $\theta_{\max} \approx \lambdabar/R_{\mathrm{N}}$, we obtain $\ln(\theta_{\max}/\theta_{\min}) \approx 2\ln(210 Z^{-1/3})$. For $\theta_{\max} = 1$, $\ln(\theta_{\max}/\theta_{\min}) = \ln(192\gamma\beta Z^{-1/3})$. We shall see that these values for $\theta_{\max}$ overestimate the effect of small-angle scattering over a wide range of parameters relevant to present-day beam propagation experiments.

B. Moliere formalism

For the case of noninteracting particles with $\partial f/\partial \mathbf{r}_\perp \equiv 0$ and $f(t=0) \propto \delta(\mathbf{v}_\perp)$, Eq. (2) can be solved exactly for arbitrary $\sigma(\theta)$ by the use of Fourier–Bessel transforms. This was first done by Moliere,[6] but the brief description given here is from a simpler derivation of Moliere's equation by Bethe.[3] The solution takes the form

$$f(\theta, t) = \int_0^\infty \eta \, d\eta \, J_0(\eta\theta) e^{N(\eta) - N_0}, \tag{8a}$$

where

$$N(\eta) = 2\pi n z \int_0^\infty \sigma(\chi) J_0(\eta\chi)\chi \, d\chi, \tag{8b}$$

and J_0 is the Bessel function of order zero. When $N_0 \gg 1$, only values of η for which $N_0 - N(\eta) \ll N_0$ contribute in Eq. (8a). For this regime, it turns out that Eq. (8b) can be evaluated analytically. To do this most conveniently, one changes variable to $\xi = \eta(nz\alpha^2 B)^{1/2}$, where B is the solution to

$$e^B/B = nz\alpha^2/(1.32\theta^2_{\min}) = N_0/1.32. \tag{9}$$

Then one can write

$$N(\xi) - N_0 = -\xi^2/4 + (\xi^2/4B)\ln(\xi^2/4) \tag{10}$$

for $0 < \xi < B^{1/2}$. Substituting this into Eq. (8a), one obtains Moliere's expansion in $1/B$:

$$f(\theta)\theta \, d\theta = \zeta \, d\zeta \, [f^{(0)}(\zeta) + B^{-1} f^{(1)}(\zeta) + B^{-2} f^{(2)}(\zeta) + \cdots], \tag{11}$$

where $\zeta = \theta/(nz\alpha^2 B)^{1/2}$ and $f^{(0)} = \exp(-\zeta^2)$. Thus, the leading term in the Moliere expansion is a Gaussian of width $\theta_{\mathrm{M}} \equiv (nz\alpha^2 B)^{1/2}$. When B is large (>10) we can write $B \approx \ln N_0 \propto \ln(z)$. So, in contrast to the result in Eq. (5), we find that the transverse temperature of the beam increases as $z \ln(z)$ instead of as z.

Comparing the widths of the Gaussians from Eqs. (5) and (11), we find that Eq. (5) overestimates the mean square transverse momentum of a beam of noninteracting particles propagating in air (see Fig. 1). Because the width of the Moliere Gaussian increases faster than linearly with z, it even-

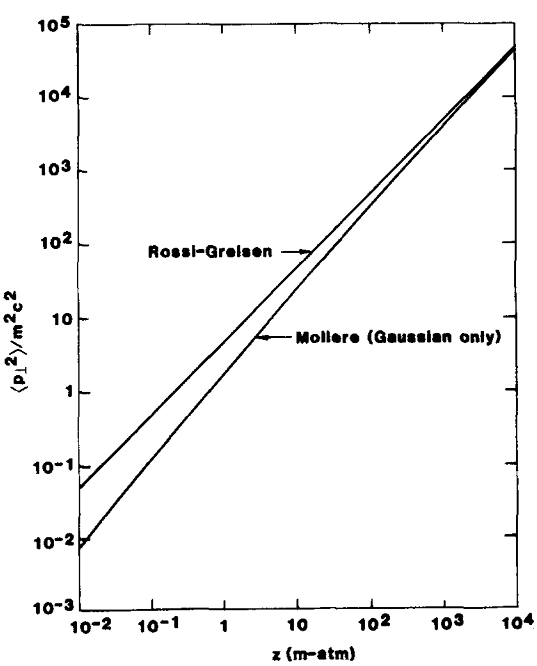

FIG. 1. Illustration of disparity between the Moliere and Rossi–Greisen predictions for the mean square transverse momentum of a beam of noninteracting particles as a function of propagation length.

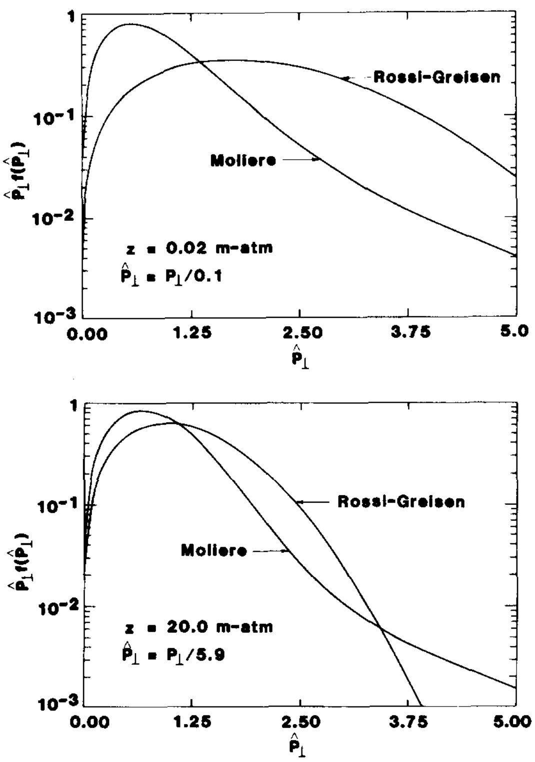

FIG. 2. The shape of the Moliere distribution relative to the Rossi–Greisen Gaussian changes as a function of propagation distance because the value of B is a function of the latter (noninteracting particles assumed).

tually catches up to the Rossi–Greisen value, but only after approximately 10^4 meter-atmospheres (m-atm).

Having derived the Moliere result, one can work backwards and deduce what value one should use for $\theta_{\max}$ in the expression for $\langle \dot{\chi}^2 \rangle$ to obtain the Moliere Gaussian width. One finds that $\theta_{\max} = \theta_{\mathrm{M}}$ is the appropriate cutoff, i.e.,

$$\langle \dot{\chi}^2 \rangle z \equiv \theta_{\mathrm{M}}^2 = 2\pi n z \int_{\theta_{\min}}^{\theta_{\mathrm{M}}} \chi^3 \, d\chi \, \sigma(\chi). \tag{12}$$

This leads to a transcendental equation for θ_{M} which is equivalent to Eq. (9). The main effect of the higher-order terms in Eq. (11) is to produce a long tail on the distribution. For large values of ζ, the expression for f goes over to the Rutherford single scattering form.[7] As a result of this tail on the distribution function, one finds that the shape of the distribution function changes as a function of propagation distance, as shown in Fig. 2. The greater the propagation distance, the closer the distribution approaches the Rossi–Greisen Gaussian, and the smaller the percentage of particles in the tail.

When self-field effects are retained, Eq. (2) becomes rather intractable. Analysis along the lines of Ref. 2 is made difficult by the fact that the rate of transfer of energy to the transverse direction is not constant, but depends on the scattered state of the beam. In Sec. III we show, however, that a semi-analytical treatment can be performed for the special case of a Bennett equilibrium.

C. Numerical algorithm

In order to look at problems where self-fields are important, we devised a numerial algorithm to implement Moliere scattering in particle simulation codes. In the algorithm, scattering angles are picked randomly from a Moliere distribution. The distribution used is one corresponding to a distance of propagation Δz much less than the characteristic length over which the beam radius changes due to scattering. To compute the Moliere distribution one has to perform time-consuming numerical integrations, so we divide the distribution into two parts,

$$P(\zeta)d\zeta = \begin{cases} f_{\mathrm{M}}(\zeta)\zeta \, d\zeta, & \zeta < \zeta_{\mathrm{cut}}, \\ \dfrac{2}{B}\dfrac{\zeta \, d\zeta}{\zeta^4}, & \zeta > \zeta_{\mathrm{cut}}; \end{cases} \tag{13}$$

where ζ_{cut} is an angle at which the Rutherford expression becomes a good approximation to the exact Moliere expression f_{M}. At $\zeta_{\mathrm{cut}} = 6$, for example, the discrepancy between the two expressions is 15%. For $\zeta < \zeta_{\mathrm{cut}}$, an array of scattering angles is computed from f_{M} once and for all on the first pass through the algorithm. For $\zeta > \zeta_{\mathrm{cut}}$, scattering angles can be obtained directly from an analytic expression, and it is thus not too time-consuming to generate new angles each time a scattering is required, especially since large-angle scatterings are relatively rare. The actual choice of a scattering angle proceeds as follows. For each particle in the beam a random number X is chosen between 0 and A where $A = \int_0^\infty P(\zeta)d\zeta$. If $X < A_{\mathrm{M}}$, where $A_{\mathrm{M}} = \int_0^{\zeta_{\mathrm{cut}}} P(\zeta)d\zeta$, then the angle corresponding to X is obtained by interpolation from the permanent array. If $X > A_{\mathrm{M}}$, the corresponding angle is computed analytically. This procedure is applied to the beam each time it advances an additional length Δz.

The length Δz cannot be made arbitrarily small, because Moliere theory breaks down rapidly for $N_0(\Delta z) < 20$. To avoid some numerical integration problems, we generally choose Δz such that $N_0 \geqslant 40$ in our algorithm. When a beam expands to the point where $\omega_\beta \sim v/L_{\mathrm{N}}$, this value of Δz can become comparable to the length scale over which the beam radius changes (see Sec. IV). We then resort to the treatment of Keil, Zeitler, and Zinn[8,9] which is specifically addressed to the regime $1 \leqslant N_0 \leqslant 20$, the so-called "plural" scattering regime. We can thus choose a suitable small Δz while maintaining accuracy.

III. SCATTERING OF BENNETT-PROFILE BEAMS

A. Preservation of Bennett profile

On the basis of a Fokker–Planck treatment of scattering, Lee[2] has shown that the Bennett equilibrium is a self-similar solution to Eq. (2) with the Bennett radius obeying the Nordsieck equation, Eq. (6). It is desirable to know if this important result carries through when Moliere scattering is employed. To study this, we inserted the scattering algorithm described in Sec. II into the one-dimensional particle simulation code SCATR. SCATR simulates the behavior of an infinitely long, axisymmetric self-pinched beam in the high-energy paraxial approximation ($v = c$, $\nu/\gamma \ll 1$). The equations which SCATR solves are (1) the Lorentz equations for the transverse motion of the individual particles and (2) Ampere's law for the self-magnetic field.

The results of simulating a 10 kA, 50 MeV beam with an initial Bennett radius of 0.5 cm are shown in Fig. 3. In Fig. 3(a) the mean radius (the radius enclosing half of the total current) is plotted, and is seen to e-fold about three times

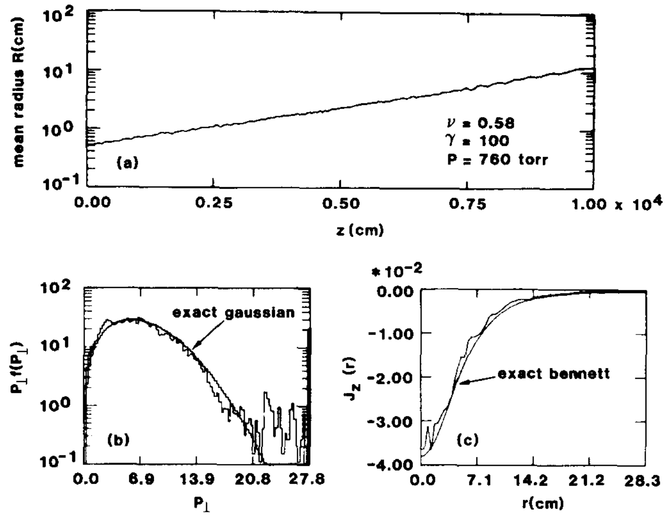

FIG. 3. Evolution of a Bennett equilibrium beam. Part (a) shows the exponential increase of the mean radius as a function of propagation distance. Parts (b) and (c) show plots of the transverse momentum distribution functions and current density after three Nordsieck lengths of propagation.

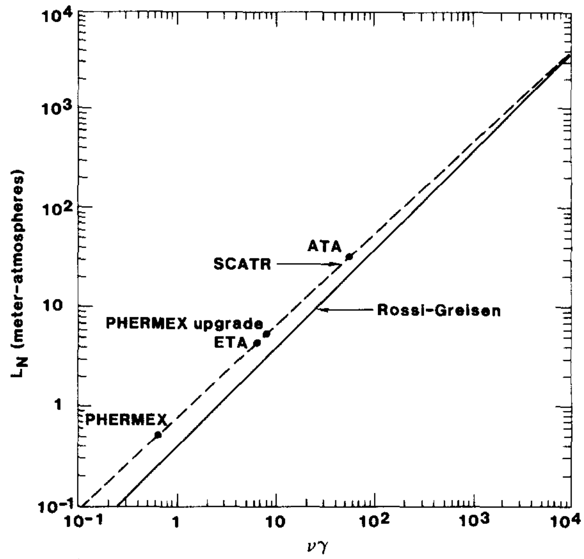

FIG. 4. Nordsieck length as a function of beam power. Over a wide range of power the Nordsieck length obtained from SCATR is significantly larger than that obtained from Eq. (7) using the Rossi–Greisen $\theta_{\max}$. The implication from some particular electron beams is indicated.

during the run. The fact that the plotted line is straight means that the radius is growing exponentially with a constant Nordsieck length L_N. In the Fokker–Planck treatment of Eq. (2), this behavior is predicted due to the facts that (1) energy is scattered into the transverse direction at a constant rate and (2) the scattered distribution is Gaussian. The numerical results suggest that these conditions are at least approximately fulfilled when Moliere scattering is applied. In Fig. 3(b) we compare the transverse distribution functions of the beam, after it has propagated three Nordsieck lengths, with an exact Gaussian. The agreement is good except in the tail. Initially, the distribution function is exactly Gaussian, as required for a Bennett equilibrium, and the non-Gaussian tail is observed to grow slowly. This tail in velocity space is a result of the long Rutherford tail on the scattering distribution. Since few particles are involved, there is no noticeable effect on the spatial current distribution, shown in Fig. 3(c). However, some loss of current can occur as a result of a few particles undergoing large-angle scattering. If a particle reaching a radial position greater than ten Bennett radii is considered lost from the beam, we find that 2%–3% of the beam current is lost per Nordsieck length. This loss rate is probably negligible for practical purposes. By the time a significant fraction of current is lost in this manner, the beam has expanded to such large radius that the quasistatic condition $v/L_N \ll \omega_\beta(R)$ no longer holds. The beam is then in a state of free expansion.

B. Evaluation of Nordsieck lengths

Equation (7) shows that for a Bennett beam, the Nordsieck length as usually defined depends only on the beam power $\nu\gamma$ (since $\gamma^2\alpha^2$ is a constant). Using SCATR we have found this to be the case with Moliere scattering also. The Nordsieck lengths obtained from SCATR are compared to those from Eq. (7) in Fig. 4. The Rossi–Greisen value for $\theta_{\max}$ was used in Eq. (7). The implications for some present-day beam machines are shown: for the Experimental Test Accelerator (ETA), the SCATR Nordsieck length is almost twice as long as that predicted by Eq. (7); for the Advanced Test Accelerator (ATA), the SCATR length is 40% longer than the Eq. (7) result. When $\nu\gamma$ reaches a value of 10^4, there is little difference between the SCATR and Rossi–Greisen results. Despite appearances, the SCATR Nordsieck length is not exactly linear in $\nu\gamma$ (see following subsection).

C. Analytic expression for Nordsieck length

The envelope equation for a self-pinched beam[5] yields a general expression for the Nordsieck length,

$$L_N = \frac{2\nu\gamma m^2c^3}{\langle dp_\perp^2/dt\rangle}, \tag{14}$$

where $\langle dp_\perp^2/dt\rangle$ is the rate at which the mean square transverse momentum of the beam changes due to scattering. As noted in Sec. III A, Moliere scattering yields (1) an approximately constant value for $\langle dp_\perp^2/dt\rangle$ and (2) an approximately Gaussian distribution in transverse momentum. Thus, to compute the value of $\langle dp_\perp^2/dt\rangle$, we throw away the non-Gaussian corrections in Moliere's equation (11). We obtain

$$\frac{1}{m^2c^2}\left\langle\frac{dp_\perp^2}{dt}\right\rangle = \gamma^2\frac{d\theta_M^2}{dt} = n\gamma^2\alpha^2\left(vB + vt\frac{dB}{dt}\right). \tag{15}$$

From Eq. (9) we obtain

$$\frac{dB}{dt} = \frac{1}{t}\frac{B}{(B-1)}. \tag{16}$$

Substituting Eqs. (15) and (16) into Eq. (14), we obtain

$$L_N = 2\nu\gamma(B-1)/n\gamma^2\alpha^2B^2. \tag{17}$$

The parameter B is a function of the transverse beam temperature, which tends to remain constant during quasistatic expansion of the beam.[2] This is because the increase in transverse energy due to scattering is balanced by the work done in expanding against the magnetic field. To compute B we

TABLE I. Comparison of Nordsieck lengths obtained from SCATR with those obtained from Eqs. (21) and (7). The value of the Moliere expansion parameter B used in Eq. (21) is also tabulated.

$\nu\gamma$	Nordsieck length (m-atm) SCATR	Eq. (21)	Eq. (7)	B
5.88 (ETA)[a]	3.9	3.9	2.3	8.8
8.0 (PHERMEX UPGRADE)[b]	5.7	5.1	3.1	9.0
58.8 (ATA)[a]	33.4	32	23.2	11.1
588	284	272	232	13.4

[a] Lawrence Livermore National Laboratory.
[b] Los Alamos National Laboratory.

use the expression for the transverse temperature of a Bennett beam, i.e., $v_{th}^2/c^2 = \nu/\gamma$, where v_{th} is the thermal velocity, so that

$$nz\alpha^2 B = \nu/\gamma. \tag{18}$$

Combining this with Eq. (9), we obtain

$$B = \ln(\nu\gamma/1.32\gamma^2\theta_{\min}^2). \tag{19}$$

Substitution into Eq. (17) gives

$$L_N = \frac{2\nu\gamma[\ln(\nu\gamma/1.32\gamma^2\theta_{\min}^2) - 1]}{n\gamma^2\alpha^2[\ln(\nu\gamma/1.32\gamma^2\theta_{\min}^2)]^2}. \tag{20}$$

If one substitutes values for α and n appropriate to air into Eq. (20), one obtains

$$L_N = 7.14\nu\gamma \frac{\ln(1090\nu\gamma)}{[\ln(2970\,\nu\gamma)]^2} \text{ m-atm.} \tag{21}$$

Equation (21) agrees to within 5% with the results of SCATR for $\nu\gamma \gtrsim 50$ and within about 10% for $\nu\gamma \lesssim 50$, as shown in Table I. The better agreement at larger values of $\nu\gamma$ is to be expected when one considers that corrections to the Gaussian in Moliere's theory enter to order $1/B$.

Since the first publication[10] of Eq. (21), a somewhat simplified derivation of this result has been given by Chambers *et al.*[11] They argue heuristically that for a self-pinched beam, $\theta_{\max}$ in Eq. (7) should be replaced by $(\nu/\gamma)^{1/2}$. This yields a good approximation to Eq. (20).

IV. COMPARISONS WITH ASTRON EXPERIMENT

The ASTRON beam at Lawrence Livermore National Laboratory was used in a study of beam expansion due to scattering some years ago.[2,12] In one experiment, the beam was injected into a tank of gas of variable pressure. The beam radius was measured two meters downstream as a function of the gas pressure. Because the ASTRON beam has a low power, it Nordsieck-expands only for a short while and then goes over into the free expansion regime. As a result, when we simulated the experiment using SCATR, we had to use a "plural" scattering algorithm, instead of a multiple scattering algorithm as discussed in Sec. II C. The experimental results for propagation in nitrogen and argon are compared to the SCATR results in Fig. 5. The agreement is good for both gases, and that for argon is an improvement on the agreement previously reported by Lee.[2] In Refs. 2 and 12, the value of $\theta_{\max}$ used is that due to Williams[13] and is approximately equal to θ_M. However, these two references assume

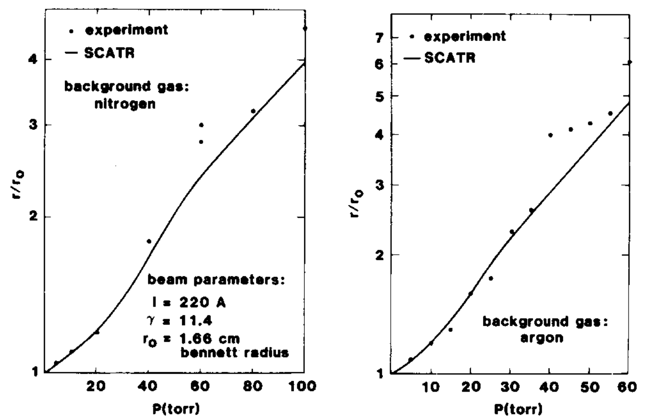

FIG. 5. Experimental results from ASTRON compared to SCATR simulations. The ratio of the beam radius 2 m from injection into the gas to the initial radius is plotted as a function of background gas pressure.

that $\theta_{\max}$ is a function of propagation distance, which is true for noninteracting particles, but not for a quasistatic self-pinched beam. For the latter, $\theta_{\max} = (\nu/\gamma)^{1/2}$ is a constant.

V. EVOLUTION OF AN ANNULAR BEAM

It has been shown by Lee[2] that under certain restrictions a self-pinched beam near equilibrium tends to assume a Bennett profile due to small-angle scattering. The rate at which this occurs was not computed, however, and to do so analytically would be laborious. SCATR is a useful tool for addressing this problem. We chose to investigate the evolution of a beam which starts out far from being a Bennett equilibrium, viz., a rotating thin annular abeam. Like the Bennett profile beams we have previously examined, the beam is assumed to be charge-neutral, nondiamagnetic, and self-pinched. The equilibrium current, magnetic field, and transverse velocity profiles are shown in Fig. 6. The value of $\nu\gamma$ for the beam is 50, which gives a predicted Nordsieck length of 27.5 m-atm in air [from Eq. (21)]. When the beam propagates, we find that it expands slower than the predicted rate for about the first Nordsieck length, and thereafter ex-

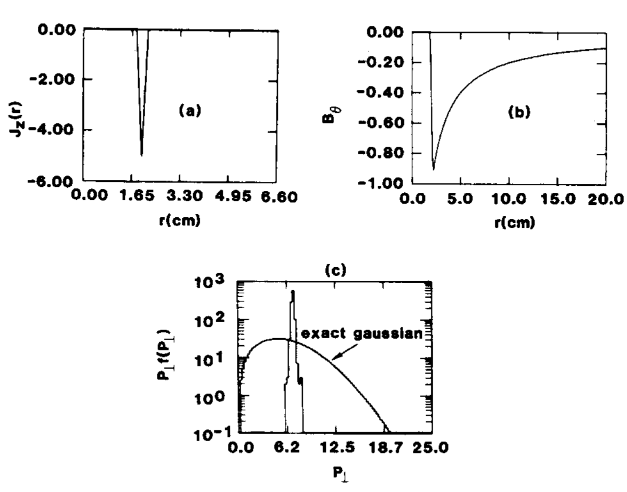

FIG. 6. Thin annular rotating beam equilibrium at $z = 0$. Parts (a) and (b) are radial profiles of the current density and magnetic field, respectively, while part (c) shows the transverse momentum distribution function.

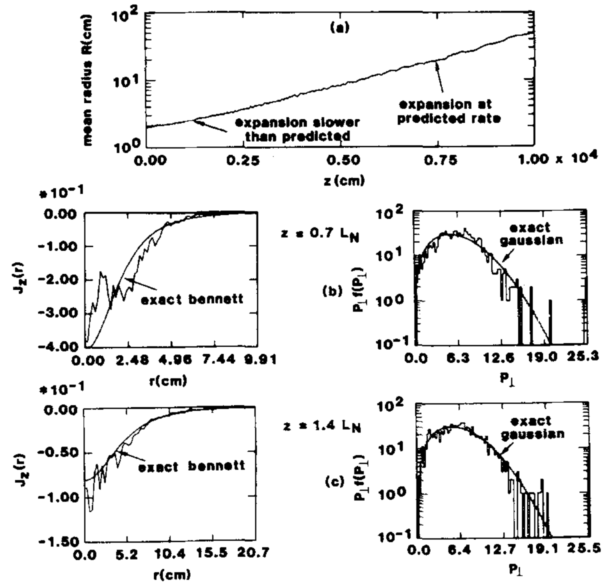

FIG. 7. Evolution of the annular beam in Fig. 6 due to small angle scattering, showing the development of a Bennett profile.

pands at the predicted rate, as shown in Fig. 7(a). If we look at what is happening to the structure of the beam during this time, we find that its annular shape is rapidly destroyed. Figure 7(b) shows that in less than a Nordsieck length, the beam has completely filled in and its transverse velocity profile is close to being Gaussian. At this point, the rotation of the beam is still sufficient to depress the current density on axis. As the beam expands further, the rotation slows down because of conservation of annular momentum and the beam profile becomes very close to being Bennett-like [Fig. 7(c)]. On the basis of these results, we think that it is reasonable to predict that any self-pinched high-energy beam with low ν/γ will acquire a Bennett profile in a distance on the order of one Nordsieck length.

VI. SUMMARY AND CONCLUSIONS

We have carried out an investigation of multiple small-angle scattering of particle beams based on the Moliere equations. Our results for Bennett equilibria obtained from a simple particle simulation code SCATR give Nordsieck lengths significantly longer than those calculated from commonly used expressions based on the less accurate Fokker–Planck formalism. On the basis of our numerical results, we are able to derive an improved analytic expression for the Nordsieck length which agrees to within 5%–10% with the numerical results, depending on the beam power. We obtain better agreement with experimental data on beam expansion from the ASTRON electron beam than that previously reported. Finally, we have studied the evolution of a non-Bennett equilibrium, namely a thin annular beam, under the influence of small-angle scattering. In a distance on the order of the Nordsieck length, the beam assumes a Bennett profile in current and a Gaussian distribution in transverse momentum. Based on this example, we tentatively conclude that all self-pinched beam equilibria with $v \simeq c$ and $\nu/\gamma \ll 1$, will evolve to a Bennett distribution in roughly one Nordsieck length.

ACKNOWLEDGMENTS

We acknowledge useful discussions with Robert Johnston, Leon Feinstein, and Keith Brueckner.

This work was supported by the Defense Advanced Research Projects Agency (DoD) under ARPA Order No. 4395.

APPENDIX: DESCRIPTION OF SCATR

The particle-in-cell code SCATR consists of a loop which alternately calculates the self-magnetic field and advances the particle positions.

Since we assume a beam current profile which is independent of the azimuthal and axial coordinates (ϕ, z), only the radial coordinate r is nonignorable. A 200-cell mesh is used to resolve the radial direction, and the bulk of the simulation particles representing the beam occupy roughly 20 cells near the origin. By increasing the mesh size Δr as the beam expands, we maintain this 10-to-1 ratio. The azimuthal magnetic field B_ϕ is computed from the discretized form of the static Ampere's Law

$$\frac{r^i B_\phi^i - r^{i-1} B_\phi^{i-1}}{\frac{1}{2}(r^i + r^{i-1})} = \frac{2\pi}{c}(J_z^i + J_z^{i-1}),$$

where the superscript i denotes the ith mesh point, $r^i = (i-1)\Delta r$, and J_z^i denotes the axial current density. The latter is obtained by interpolating the current contribution of each simulation particle onto the mesh points. Usually, one thousand particles are used to model the beam.

To treat the particle dynamics, we first advance the momenta in locally Cartesian coordinates [Eq. (A1)], then advance the particle positions [Eq. (A2)], and finally transform the momenta back to cylindrical coordinates [Eqs. (A3) and (A4)]. The algorithm is as follows:

$$(P_1 - P_r^{N-1})/\Delta t = e(v/c)B_\phi^{N-1/2}, \tag{A1}$$

$$r^{N+1/2} = \left[\left(\frac{P_1 \Delta t}{\gamma m} + r^{N-1/2}\right)^2 + \left(\frac{P_\phi^{N-1}\Delta t}{\gamma m}\right)^2\right]^{1/2}, \tag{A2}$$

$$P_r^N = \frac{P_1 r^{N-1/2}}{r^{N+1/2}} + [P_1^2 + (P_\phi^{N-1})^2]\frac{\Delta t}{\gamma m r^{N+1/2}}, \tag{A3}$$

$$P_\phi^N = P_\phi^{N-1} r^{N-1/2}/r^{N+1/2}, \tag{A4}$$

where N denotes the number of time steps, Δt is the time step, P_r, P_ϕ are the particle momenta, and $B_\phi^{N-1/2}$ is obtained by interpolating the field from the mesh points to the particle positions. The effect of collisions on the particle momenta is taken into account in the manner described in Sec. II.

[1] W. H. Bennett, Phys. Rev. **45**, 890 (1934).
[2] E. P. Lee, Phys. Fluids **19**, 60 (1976).
[3] H. A. Bethe, Phys. Rev. **89**, 1256 (1953).
[4] B. Rossi and K. Greisen, Rev. Mod. Phys. **13**, 240 (1941).
[5] E. P. Lee and R. K. Cooper, Part. Accel. **7**, 83 (1976).

[6]G. Moliere, Z. Naturforsch. A **3**, 78 (1948).
[7]See, e.g., J. D. Jackson, *Classical Electrodynamics* (Wiley, New York, 1962), p. 452.
[8]E. Keil, E. Zeitler, and W. Zinn, Z. Naturforsch. A **15**, 1031 (1960). (A discussion of their work is given in Ref. 9.)
[9]W. T. Scott, Rev. Mod. Phys. **35**, 231 (1963).
[10]T. P. Hughes and B. B. Godfrey, AMRC-R-389, Mission Research Corporation, Albuquerque, 1982.
[11]F. W. Chambers, S. Yu, and E. P. Lee (private communication).
[12]R. J. Briggs, R. E. Hester, E. J. Lauer, E. P. Lee, and R. L. Spoerlein, Phys. Fluids **19**, 1007 (1976).
[13]E. J. Williams, Proc. R. Soc. London Ser. A **169**, 531 (1939).